



Title	Deprotonation of a dinuclear copper complex of 3,5-diamino-1,2,4-triazole for high oxygen reduction activity
Author(s)	Kato, Masaru; Kimijima, Ken'ichi; Shibata, Mari; Notsu, Hideo; Ogino, Kazuya; Inokuma, Kiyoshi; Ohta, Narumi; Uehara, Hiromitsu; Uemura, Yohei; Oyaizu, Nobuhisa; Ohba, Tadashi; Takakusagi, Satoru; Asakura, Kiyotaka; Yagi, Ichizo
Citation	Physical chemistry chemical physics, 17(14), 8638-8641 https://doi.org/10.1039/c4cp05595k
Issue Date	2015-03-03
Doc URL	http://hdl.handle.net/2115/60824
Type	article (author version)
File Information	PCCP_revisedManuscript_CuHdatrz_XANES_final_nohighlight.pdf



[Instructions for use](#)

COMMUNICATION

Deprotonation of a dinuclear copper complex of 3,5-diamino-1,2,4-triazole for high oxygen reduction activity†

Cite this: DOI: 10.1039/x0xx00000x

Received 00th January 2012,
Accepted 00th January 2012

DOI: 10.1039/x0xx00000x

www.rsc.org/

Masaru Kato,^{a,b} Ken'ichi Kimijima,^{c,1} Mari Shibata,^c Hideo Notsu,^c Kazuya Ogino,^c Kiyoshi Inokuma,^c Narumi Ohta,^{c,1} Hiromitsu Uehara,^d Yohei Uemura,^{d,1} Nobuhisa Oyaizu,^b Tadashi Ohba,^d Satoru Takakusagi,^d Kiyotaka Asakura^{d,*} and Ichizo Yagi^{a,b,c,*}

A dinuclear copper(II) complex of 3,5-diamino-1,2,4-triazole is one of the highly active copper-based catalysts for the oxygen reduction reaction (ORR) in basic solution. Our *in situ* X-ray absorption near edge structure measurements revealed that deprotonation from the triazole ligand might cause coordination geometrical changes, resulting in enhancement of the ORR activity.

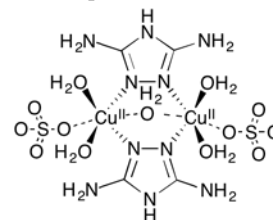
Polymer electrolyte fuel cells (PEFCs) generate electricity from oxygen and hydrogen, where only water is produced without the formation of any toxic or greenhouse gases. PEFCs are sustainable power sources for mobile phones, laptop computers and vehicles, and have great potential to shift away from the fossil-fuel economy we have today toward a carbon-emission-free economy, where hydrogen will be used as an energy source. To develop practical PEFCs we need to overcome many technical obstacles, and one well-known bottleneck for the widespread applications of PEFCs is the development of low-cost catalysts for the oxygen reduction reaction (ORR) at the cathode. The best-known electrocatalyst for ORR is carbon-supported platinum metal.^{1–4} Despite extensive efforts in searching for efficient Pt-based catalysts, platinum is scarce and the Pt-based cathodes still require a large overpotential of > 200 mV for ORR. It is highly desirable to find low-cost electrocatalysts that can fulfill demands in PEFCs.

In nature multicopper oxidases (MCOs) such as laccases are able to catalyze the ORR with great efficiency.⁵ MCOs reduce oxygen to water at their multi-nuclear copper active site with almost no overpotential (ca. 20 mV).^{6–10} It is most unlikely that the enzymes would be used as biocathodes in practical PEFCs, since the enzymes are easily denatured and their footprints are large (ca. 160 nm³ for laccase),¹¹ resulting in low stability and power outputs, respectively. The active site structures of MCOs, however, have inspired us to design artificial copper-based ORR catalysts, and many bio-inspired electrocatalysts have extensively been studied.^{12–15}

A bio-inspired dinuclear copper(II) complex of 3,5-diamino-1,2,4-triazole (Cu-Hdatrz, **Scheme 1**)¹⁶ supported on a carbon black shows high ORR activities in basic solutions.¹⁷ Although many studies on the Cu-Hdatrz catalyst have been done, for example, its tolerance to poisoning ions¹⁸ and its ORR activity in a lipid layer,¹⁹ its detailed

catalytic mechanism has not been understood yet. The investigation of the chemical nature of Cu-Hdatrz under reaction conditions will give us insights into such high ORR activities in basic solutions, and will facilitate further development of bio-inspired ORR catalysts.

Here we report electrochemical and *in situ* X-ray absorption fine structure (XAFS) studies of the carbon-supported Cu-Hdatrz under neutral and basic conditions. *In situ* XAFS is a powerful technique to probe the electronic structure or coordination geometry of metal-based electrocatalysts under catalytic conditions.^{20–22} In this work we studied X-ray absorption near-edge structure (XANES) spectra of the Cu-Hdatrz at various bias potentials under neutral and basic conditions (pH 7, 10 and 13) to understand relationships between deprotonation of the active species and the ORR activity.



Scheme 1 Molecular structure of the dinuclear copper(II) complex of 3,5-diamino-1,2,4-triazole (Cu-Hdatrz).

A carbon black-supported Cu^{II}-Hdatrz was synthesized from CuSO₄·5H₂O, Hdatrz and Ketjenblack ECP300 (KB), based on the method in the literature with slight modifications (See ESI†).¹⁷ KB was a carbon black with a relatively high BET surface area (813 m² g⁻¹), compared to Vulcan (247 m² g⁻¹), which was used as a carbon support in the original catalyst.¹⁷ Carbon supports with high surface areas, in principle, allow us to load well-dispersed catalysts, which are suitable for fluorescent XANES measurements with high data quality.

Cyclic voltammograms (CVs) of the copper(II) complex of Hdatrz supported on KB (Cu/KB) were recorded under Ar to understand the redox behavior of Cu/KB in a non-catalytic condition (**Fig. 1**). At pH 7 an oxidation wave at +0.73 V vs RHE and a reduction wave at +0.39 V vs RHE were observed, and these waves were assigned to an oxidation wave to Cu^{II} and a reduction wave to Cu^I, respectively. The peak separation

between these peaks was approximately 0.33 V, which was much greater than 0 V for electrochemical active species strongly adsorbing on electrode surfaces, indicating that the electrochemical redox behavior of Cu-Hdartz was irreversible. We also recorded CVs of Cu/KB at pH 4, pH 10 and pH 13, and obtained the similar results on the peak separation. Thus, the redox reaction of Cu^{II} -Hdartz may involve structural changes such as geometrical changes around the metal center.

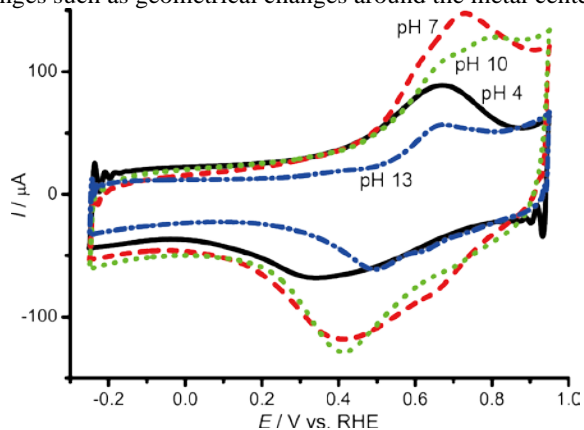


Fig. 1 CVs of Cu/KB in Britton-Robinson buffered aqueous solutions (0.04 M) containing 0.1 M NaClO_4 at pH 4 (solid line in black), 7 (dashed line in red), 10 (dotted line in green) and pH 13 (alternate long and short dashed line in blue). All CVs shown here were recorded at a sweep rate of 100 mV s^{-1} under Ar.

The ORR activity of Cu/KB was studied using rotating ring disc electrodes (RRDEs) in buffered aqueous solutions at pH 4, 7, 10 and 13. Linear sweep voltammograms of Cu/KB were recorded at 1600 rpm under oxygen (Fig. 2). An onset potential of Cu/KB for ORR was observed at +0.77 V vs RHE at pH 7 and a diffusion-limited current reached ca. -1.0 mA . A quite similar ORR activity was observed for Cu-Hdartz on Vulcan under the same condition (Fig. S1, ESI[†]), suggesting that there was no obvious effect of the carbon supports (KB and Vulcan) on catalytic activity. The ring current of Cu/KB is less than $5 \mu\text{A}$ at pH 7, indicating that almost no hydrogen peroxide generation during ORR. Thus, Cu/KB is able to selectively reduce molecular oxygen to water.

The ORR activity of Cu/KB depends on pH, and Cu/KB is more active in the basic solutions than in the neutral solution: the onset potentials for ORR were shifted in the positive direction with increasing pH, and the plot of the onset potential against pH gave a linear relationship with a slope of 26 mV / pH (Fig. 2C), which is equivalent to -33 mV / pH using a pH-independent reference electrode. This value is approximately half the value of -60 mV / pH , implying that the rate-limiting step involves the transfer of two electrons and one proton. The same results were reported on Cu^{II} -Hdartz supported on a carbon black of Vulcan, where the reduction of two copper centers and the concomitant protonation of a bridging OH^- or O^{2-} ligand.¹⁷ These results suggest that carbon supports may not influence the ORR mechanism of Cu-Hdartz in the pH range from 4 to 13.

In situ XANES spectra of Cu/KB were recorded at pH 7, 10 and 13 in catalytic (under O_2) and non-catalytic conditions (under N_2) to gain insights into active species during ORR. The potential dependent XANES spectra of Cu/KB are shown in Fig. 3. The spectra have isosbestic points, indicating that Cu^{II} -Hdartz was electrochemically converted to one reduced species,

and a characteristic peak appeared at $\sim 8981 \text{ eV}$ in the edge region upon the electrochemical reduction. This peak is assigned to the $1s \rightarrow 4p_\pi$ transition of a Cu^{I} complex.²²⁻²⁴ Thus, Cu^{II} -Hdartz was electrochemically reduced and converted to the Cu^{I} species.

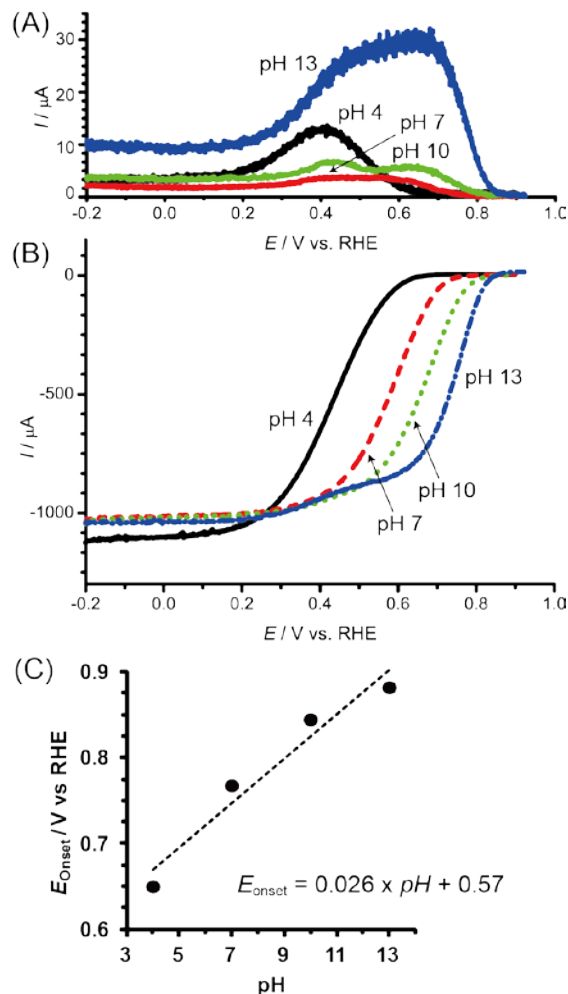


Fig. 2 (A) Ring and (B) disc current of linear sweep voltammograms of Cu/KB using a RRDE (disc: glassy carbon with 0.196 cm^2 ; ring: Pt) at 1600 rpm at pH 4 (black), pH 7 (red), pH 10 (green) and pH 13 (blue) under oxygen. The voltammograms were recorded at a sweep rate of 20 mV s^{-1} scanning in the positive direction. Britton-Robinson buffered aqueous solution (0.04 M) containing 0.1 M NaClO_4 was used as electrolyte solution. A constant bias potential of 1.2 V vs RHE was applied to the Pt ring electrode. (C) A plot of onset potential for ORR vs. pH. The plot gave a linear relationship with $E_{\text{onset}} = 0.026 \times \text{pH} + 0.57$.

Linear combination fitting analysis was performed for the XANES spectra of Cu/KB, and percentages of Cu^{I} species were calculated, assuming that all Cu^{II} -Hdartz molecules were reduced at -0.25 V vs RHE at pH 7, at -0.08 V vs RHE at pH 10 and at $+0.09 \text{ V vs RHE}$ at pH 13 (Insets in Fig. 3). Although at pH 7 there were no difference between the amounts of Cu^{I} under N_2 and O_2 (Fig. 3A), more amounts of Cu^{I} were observed under N_2 than those under oxygen at pH 10 (Fig. 3B) and pH 13 (Fig. 3C). Thus, it is clear that the electrochemical behavior

of Cu-Hdatrz under basic conditions is different from that under the neutral condition.

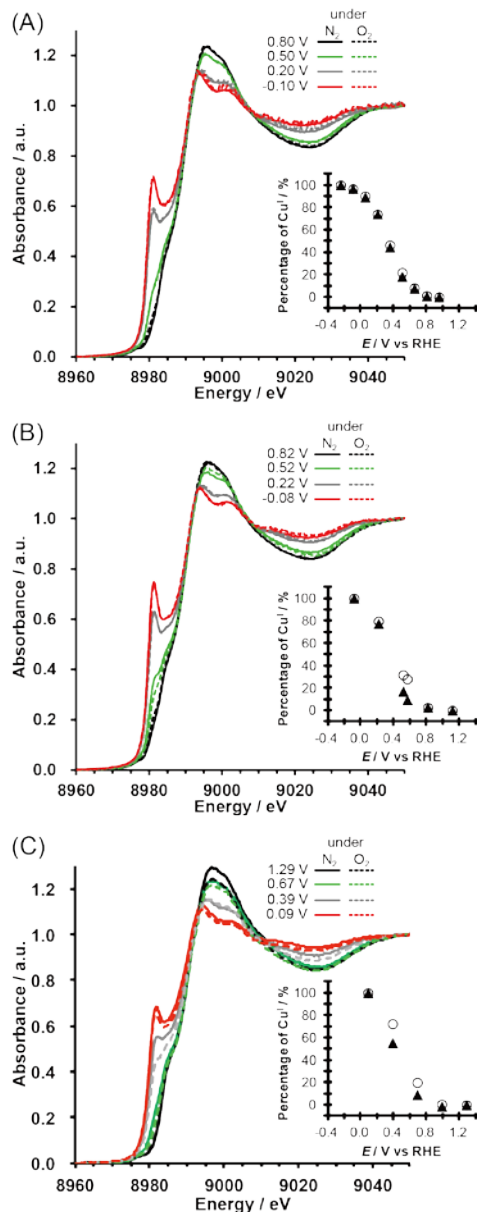
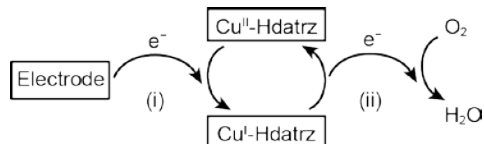


Fig. 3 *In situ* fluorescent XANES spectra of Cu/KB (A) at pH 7, (B) at pH 10 and (C) pH 13. The solid line and dashed lines indicate the XANES spectra that were recorded under nitrogen and oxygen, respectively. Insets: plots of percentages of Cu^I vs applied potential (open circle: under nitrogen; filled triangle: under oxygen). The percentages were calculated based on the results of the linear combination analysis of the XANES spectra of Cu/KB and fully reduced Cu/KB.

Considering the amounts of Cu^I calculated (Fig. 3) and two simplified electron transfer steps (Scheme 2), we concluded that the second electron transfer might be faster in the basic solutions than that in the neutral solution. The first step is the electron transfer from the electrode or KB to the Cu^{II}-Hdatrz complex and the second step is the electron transfer from the Cu^I species to molecular oxygen (the ORR step). The XANES spectra at pH 7 under N₂ and O₂ exhibited the same relative amounts of Cu^I at each potential, indicating that Cu^{II}-Hdatrz

can be immediately reduced to the Cu^I species even in the presence of oxygen. At pH 10 and pH 13 less relative amounts of Cu^I were observed under O₂ than those under N₂, suggesting that the ORR was faster than the reduction of Cu^{II}-Hdatrz by the electrode or KB at pH 10. The second electron transfer (the ORR step) may be faster in the basic solutions than that in the neutral solution, which is consistent with the high ORR activity observed in the basic solution (Fig. 2).



Scheme 2 Simplified electron transfer steps in the Cu-Hdatrz/KB system: (i) electron transfer from the electrode/KB to Cu^{II}-Hdatrz and (ii) electron transfer from Cu^I-Hdatrz to O₂ (the ORR step).

Since XANES spectra are sensitive to coordination geometrical changes around the element measured, the XANES spectra of Cu/KB recorded at pH 7, pH 10 and pH 13 were overlaid to compare the shape of them (Fig. 4). Although the almost same shape of the spectra was observed at pH 7 and pH 10 in the same oxidation state, the XANES spectra at pH 13 were different from those at pH 7 and pH 10, indicating that the coordination geometries of the Cu^{II} and Cu^I centers were the same in the pH range from pH 7 to pH 10, but these might be different at pH 13. Furthermore, spectral differences were observed between the XANES spectra under nitrogen and oxygen at pH 13 (Fig. S2, ESI†). Since a pK_a value of Hdatrz was reported to be 12.12,²⁵ it is most likely that deprotonation occurred from the Hdatrz ligands at pH 13. Thus, deprotonation from the Cu-Hdatrz in basic solutions may affect the electronic state of the Hdatrz ligands and induce coordination geometrical changes, resulting in highly active ORR catalyst in basic solutions.

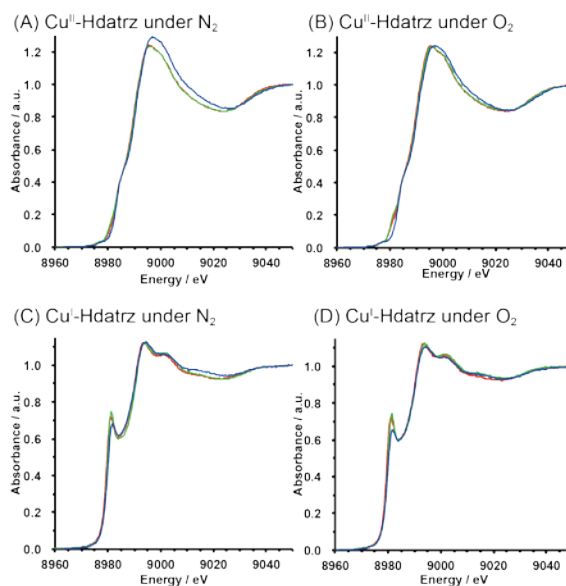


Fig. 4 *In situ* XANES spectra of Cu/KB in the oxidation state of Cu^{II} (A) under N₂ and (B) under O₂, and in the oxidation state of Cu^I (C) under N₂ and (D) under O₂. The red, green and blue traces indicate the spectra recorded at pH 7, pH 10 and pH 13, respectively. Bias potentials applied are as follows: +0.95 V

vs RHE at pH 7, +1.11 V vs RHE at pH 10 and +1.29 V vs RHE at pH 13 for Cu^{II}; -0.25 V vs RHE at pH 7, -0.08 V vs RHE at pH 10 and +0.09 V vs RHE at pH 13 for Cu^I.

In summary, the electrochemical ORR activity Cu/KB was studied in the neutral and basic aqueous solutions using the *in situ* electrochemical XANES techniques. Our electrochemical studies revealed that the faster ORR kinetics of Cu/KB resulted in the higher ORR catalytic activity under the basic conditions, compared to that under the neutral condition. The coordination geometry at pH 13 was different from those at pH 7 and pH 10, and this difference might be caused by deprotonation of the Hdatrz ligand. The structural information on the deprotonated Cu^I species or O₂-bound intermediates in basic solutions may be a key to understand the high ORR activity of Cu/KB or to design highly active Cu-based ORR catalysts.

Further *in situ* XAFS studies on the Cu-Hdatrz complex are under way to obtain more detailed structural information in basic solutions.

Acknowledgements

This work has been supported by NEDO and performed under the approval of the Photon Factory Program Advisory Committee (Proposal No. 2010G200 & 2013G173).

Notes and references

^a Faculty of Environmental Earth Science, Hokkaido University, N10W5, Kita-ku, Sapporo 060-0810 Japan. E-mail: iyagi@ees.hokudai.ac.jp

^b Graduate School of Environmental Science, Hokkaido University, N10W5, Kita-ku, Sapporo 060-0810 Japan.

^c Fuel Cell Cutting-Edge Center - Technology Research Association (FC-Cubic, TRA), 2-3-26 Aomi, Koto-ku, Tokyo 135-0064 Japan.

^d Catalysis Research Center, Hokkaido University, N21W10, Kita-ku, Sapporo, Hokkaido 001-0021 Japan.

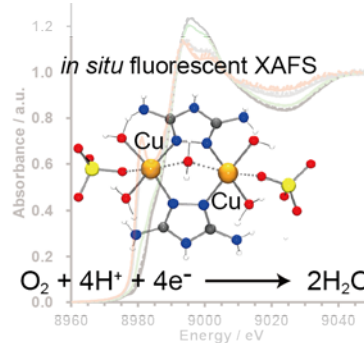
^f Present addresses: Institute of Materials Structure Science, High Energy Accelerator Research Organization, KEK, Oho 1-1, Tsukuba, Ibaraki, 305-0801, Japan (K.K.); Environment and Energy Materials Division, National Institute for Materials Science, 1-1 Namiki, Tsukuba, Ibaraki, 305-0044 Japan (N.O.); Division of Electronic Structure, Department of Materials Molecular Science, Institute for Molecular Science, Myodaiji, Okazaki 444-8585, Japan (Y.U.).

† Electronic Supplementary Information (ESI) available: Experimental section and Figures on our spectroelectrochemical cell, electrochemical ORR and *in situ* XANES spectra. See DOI: 10.1039/c000000x/

1. A. A. Gewirth and M. S. Thorum, *Inorg. Chem.*, 2010, **49**, 3557-3566.
2. S. Guo, S. Zhang and S. Sun, *Angew. Chem. Int. Ed.*, 2013, **52**, 8526-8544.
3. I. Katsounaros, S. Cherevko, A. R. Zeradjanin and K. J. J. Mayrhofer, *Angew. Chem. Int. Ed.*, 2014, **53**, 102-121.
4. A. Morozan, B. Josselme and S. Palacin, *Energy Environ. Sci.*, 2011, **4**, 1238-1254.
5. J. A. Cracknell, K. A. Vincent and F. A. Armstrong, *Chem. Rev.*, 2008, **108**, 2439-2461.
6. C. F. Blanford, R. S. Heath and F. A. Armstrong, *Chem. Commun.*, 2007, 1710-1712.
7. N. Mano, V. Soukharev and A. Heller, *J. Phys. Chem. B*, 2006, **110**, 11180-11187.

8. P. Olejnik, B. Palys, A. Kowalczyk and A. M. Nowicka, *J. Phys. Chem. C*, 2012, **116**, 25911-25918.
9. V. Climent, Y. Fu, S. Chumillas, B. Maestro, J.-F. Li, A. Kuzume, S. Keller and T. Wandlowski, *J. Phys. Chem. C*, 2014, **118**, 15754-15765.
10. M. S. Thorum, C. A. Anderson, J. J. Hatch, A. S. Campbell, N. M. Marshall, S. C. Zimmerman, Y. Lu and A. A. Gewirth, *J. Phys. Chem. Lett.*, 2010, **1**, 2251-2254.
11. K. Piontek, M. Antorini and T. Choinowski, *J. Biol. Chem.*, 2002, **277**, 37663-37669.
12. D. Das, Y.-M. Lee, K. Ohkubo, W. Nam, K. D. Karlin and S. Fukuzumi, *J. Am. Chem. Soc.*, 2013, **135**, 4018-4026.
13. C. C. L. McCrory, X. Ottenwaelde, T. D. P. Stack and C. E. D. Chidsey, *J. Phys. Chem. A*, 2007, **111**, 12641-12650.
14. M. A. Thorseth, C. S. Letko, T. B. Rauchfuss and A. A. Gewirth, *Inorg. Chem.*, 2011, **50**, 6158-6162.
15. M. A. Thorseth, C. E. Tornow, E. C. M. Tse and A. A. Gewirth, *Coord. Chem. Rev.*, 2013, **257**, 130-139.
16. E. Aznar, S. Ferrer, J. Borrás, F. Lloret, M. Liu-Gonzalez, H. Rodriguez-Prieto and S. Garcia-Granda, *Eur. J. Inorg. Chem.*, 2006, **2006**, 5115-5125.
17. M. S. Thorum, J. Yadav and A. A. Gewirth, *Angew. Chem. Int. Ed.*, 2009, **48**, 165-167.
18. M. S. Thorum, J. M. Hankett and A. A. Gewirth, *J. Phys. Chem. Lett.*, 2011, **2**, 295-298.
19. C. J. Barile, E. C. M. Tse, Y. Li, T. B. Sobyra, S. C. Zimmerman, A. Hosseini and A. A. Gewirth, *Nat. Mater.*, 2014, **13**, 619-623.
20. K. A. Kuttiyiel, K. Sasaki, Y. Choi, D. Su, P. Liu and R. R. Adzic, *Energy Environ. Sci.*, 2012, **5**, 5297-5304.
21. Y. Gorlin, B. Lassalle-Kaiser, J. D. Benck, S. Gul, S. M. Webb, V. K. Yachandra, J. Yano and T. F. Jaramillo, *J. Am. Chem. Soc.*, 2013, **135**, 8525-8534.
22. F. Giordano, E. Borfecchia, K. A. Lomachenko, A. Lazzarini, G. Agostini, E. Gallo, A. V. Soldatov, P. Beato, S. Bordiga and C. Lamberti, *J. Phys. Chem. Lett.*, 2014, **5**, 1552-1559.
23. L. S. Kau, D. J. Spira-Solomon, J. E. Penner-Hahn, K. O. Hodgson and E. I. Solomon, *J. Am. Chem. Soc.*, 1987, **109**, 6433-6442.
24. E. I. Solomon, D. E. Heppner, E. M. Johnston, J. W. Ginsbach, J. Cirera, M. Qayyum, M. T. Kieber-Emmons, C. H. Kjaergaard, R. G. Hadt and L. Tian, *Chem. Rev.*, 2014, **114**, 3659-3853.
25. T. P. Kofman, *Russ. J. Org. Chem.*, 2001, **37**, 1158-1168.

Table of Contents



In situ XAFS studies on a copper catalyst revealed that deprotonation from the triazole ligand might cause the coordination geometrical changes, resulting in enhancement of the oxygen reduction reaction activity.